

# Predicted Infrared and Raman Spectra for Neutral $\text{Ti}_8\text{C}_{12}$ Isomers

Tunna Baruah<sup>1,2</sup>, Mark R. Pederson<sup>2</sup>, M. L. Lyn<sup>3</sup> and A. W. Castleman Jr.<sup>3</sup>

<sup>1</sup>*Department of Physics, Georgetown University, Washington, DC 20057*

<sup>2</sup>*Center for Computational Materials Science, Code 6390,  
Naval Research Laboratory, Washington, DC 20375\* and*

<sup>3</sup>*Departments of Chemistry and Physics, Pennsylvania State University, University Park, PA 16802*

(Dated: November 2, 2018)

Using a density-functional based algorithm, the full IR and Raman spectra are calculated for the neutral  $\text{Ti}_8\text{C}_{12}$  cluster assuming geometries of  $T_h$ ,  $T_d$ ,  $D_{2d}$  and  $C_{3v}$  symmetry. The  $T_h$  pentagonal dodecahedron is found to be dynamically unstable. The calculated properties of the relaxed structure having  $C_{3v}$  symmetry are found to be in excellent agreement with experimental gas phase infrared results, ionization potential and electron affinity measurements. Consequently, the results presented may be used as a reference for further experimental characterization using vibrational spectroscopy.

## I. INTRODUCTION

In 1992, Castleman and co-workers<sup>1,2</sup> discovered the first of a family of magic number clusters, called metallocarbohedrenes, amidst a metal-carbon cluster distribution produced using a laser plasma reactor source. Metallocarbohedrenes, or Met-Cars for short, are clusters of stoichiometry  $\text{M}_8\text{C}_{12}$  ( $\text{M} = \text{V}, \text{Zr}, \text{Hf}, \text{Ti}, \text{Nb}, \text{Mo}, \text{Fe}, \text{Cr}$ )<sup>1,2,3,4</sup> or  $\text{Ti}_{8-x}\text{M}_x\text{C}_{12}$  ( $\text{M} = \text{Zr}, \text{Hf}, \text{Nb}, \text{Mo}, \text{Ta}, \text{W}, \text{Si}, \text{Y}, \text{Nb}, \text{Mo}, \text{Ta}, \text{W}$ )<sup>5,6,7</sup>. Bearing an unusual 2:3 metal-carbon reduced stoichiometric ratio, a pentagonal dodecahedral cage structure having  $T_h$  point group symmetry was proposed by Castleman to account for ligand titration experiments which suggested that the eight metal atoms had similar coordination<sup>1</sup>. Shortly thereafter, Dance<sup>8,9</sup> proposed a tetracapped tetrahedron of  $T_d$  symmetry and later showed that the  $T_h$  dodecahedron was higher in energy by 15 eV. Other geometries have also been proposed including structures belonging to the  $C_{3v}$  point group<sup>10,11,12,13</sup>. Comparison of the drift time of mass selected  $\text{Ti}_8\text{C}_{12}^+$  with calculated mobilities for various structures reinforces the proposed hollow cage structures instead of more closely packed cubic structures<sup>14,15</sup>.

Despite the considerable amount of interest in the chemical and physical properties of Met-Cars, the equilibrium geometry is still not known<sup>13</sup>. If these  $\text{M}_8\text{C}_{12}$  clusters are to be realized as new materials, production and isolation in macroscopic quantities is imperative. Early experiments by Castleman *et al.* showed that Met-Cars exposed to air were stable for short periods of time possibly due to protection by soot<sup>16</sup>. Most recently, Selvan and Pradeep also approached the bulk synthesis problem, using an arc-discharge<sup>17</sup>. Infrared spectra of the soot after exposure to air over the course of 30 minutes showed the disappearance of a band at  $665\text{ cm}^{-1}$  and the emergence of others at  $1457$ ,  $1122$ , and  $872\text{ cm}^{-1}$ . The “appearing” bands were assigned to methylene wagging, C-C bond stretching, and methylene rocking modes, respectively. As discussed below, the highest energy “appearing” mode ( $1457\text{ cm}^{-1}$ ) also is close to the energy range associated with Met-Cars. Time-lapse variations across IR spectra cannot be used to declare the presence of a “new” material when the disappearing or emerging

peak(s) are not known or expected to be signatures of the species under investigation.

Recently, the infrared spectra for neutral  $\text{Ti}_8\text{C}_{12}$ , as well as for  $\text{Ti}_8\text{C}_{11}$  and  $\text{Ti}_{14}\text{C}_{13}$ , have been measured in the gas phase by infrared multiphoton excitation using a pulsed linear accelerator<sup>18</sup>. Though the measurement represents the vibrational signature for a free Met-Car, it serves as the first available experimental reference applicable for use in the identification of the presence of  $\text{Ti}_8\text{C}_{12}$  in unpurified samples. Recently, Gueorguiev and Pacheco<sup>19</sup> have calculated the infrared absorption spectrum for the  $\text{Ti}_8\text{C}_{12}$ . Their calculations have shown the Met-Cars with distorted  $T_d$  geometry to be the lowest energy ones while the experimental IR-absorption spectrum compares better with the calculated spectrum for the  $D_{2d}$  structure. This is clearly a finite temperature effect. However, the width of the experimental peak near  $1400\text{ cm}^{-1}$  is much larger than predicted by the above mentioned article. Neither the experimental<sup>18</sup> or theoretical<sup>19</sup> works give strong evidence that there is Met-Car infrared intensity near the  $665\text{ cm}^{-1}$  range. Therefore an additional calculation aimed at this question is useful. Another motivation of the present work is to identify the symmetry of the lowest energy structure within the density functional theory. A comparison of the theoretical IR absorption spectra with experiment will certainly be helpful in this regard. However, due to the fact that the existing experimental measurements were carried out at finite temperature, the characterization of the ground state structure through IR measurement may be unreliable. We show in the following that at finite temperature in which the experiments are carried out, the spectra is a mixture of low lying isomers leading to a large width of the high frequency peak. In this paper, we present the complete vibrational modes for a  $D_{2d}$  structure and a  $C_{3v}$  trigonal pyramid  $\text{Ti}_8\text{C}_{12}$  as determined from all-electron density functional studies. Apart from the IR absorption spectrum, we also present our calculated Raman scattering spectrum for these structures. This is the first calculated Raman spectrum of  $\text{Ti}_8\text{C}_{12}$ . The reliability of our predicted Raman frequencies can be assessed based on agreement between the calculated IR spectrum and the gas phase IR results or other exper-

imentally determined properties.

## II. COMPUTATIONAL DETAILS

The geometrical and electronic structures of  $\text{Ti}_8\text{C}_{12}$  molecule of different structures were studied using density functional theory<sup>20</sup>. The calculations were performed with the NRLMOL code<sup>21</sup> within the generalized gradient approximation to the exchange-correlation energy<sup>22</sup>. The Kohn-Sham orbitals were expanded in a basis of linear combination of atomic orbitals where each orbital is expanded in a Gaussian basis set centered on the atoms. An optimized basis set<sup>23</sup> was employed to speed up the calculations. The basis for the Ti atom consists of 7 s-type, 5 p-type and 4 d-type orbitals each of which are constructed from a linear combination of 19 Gaussians. For C atom, 5 s-type, 4 p-type and 3 d-type functions were used which in turn are composed of 12 Gaussians. A variational integration mesh was used for the analytical computation of the potential<sup>24</sup>. Spin-polarized calculations were performed taking all electrons into account. The optimization of the clusters was symmetry adapted. The massively parallel version of the code<sup>25</sup> was used and the calculations were carried out on a cluster of PCs. The geometry optimizations were carried out by using the limited-memory Broyden-Fletcher-Goldfarb-Shanno (LBFGS) scheme of minimization. The geometry optimizations were carried till the forces on the atoms were below 0.001 a.u. For each geometry, the self-consistency cycle was carried out till the energy differences were less than 0.000001 a.u.

To calculate the vibrational frequencies, a dynamical matrix was constructed by first displacing the atoms by  $\pm 0.08$  a.u. and calculating the forces. The vibrational frequencies of the molecules were calculated by a direct diagonalization of the dynamical matrix. The details of the method can be found in Ref.<sup>26</sup>. The Raman and infrared intensities were obtained from the derivatives of the dipole moment and the polarizability tensor which in turn were obtained by applying an electric field of strength 0.005 a.u.. For a high precision calculation of the vibrational frequencies and the Raman and IR intensities, the energies of the displaced geometries were converged to a tolerance of  $1.0 \times 10^{-8}$  a.u..

## III. RESULTS AND DISCUSSION

The earlier reports of the Met-Car structure have shown the  $\text{Ti}_8\text{C}_{12}$  clusters with a  $T_d$  geometry to be lower in energy than the one with  $T_h$  symmetry. It may be recalled here that Dance<sup>9</sup> have shown a barrierless reaction pathway between  $T_h$  and the  $T_d$  structures he considered. The path was constrained with the  $D_2$  symmetry. On the other hand, Chen et al.<sup>11</sup> have proposed a  $D_{2d}$  structure to be more strongly bound. To obtain possi-

ble candidate structures for the low energy isomers, we have performed the geometry optimizations for different structures with  $T_d$ ,  $T_h$ ,  $C_{3v}$ ,  $D_{2d}$ ,  $D_{2h}$  and  $D_2$  point group symmetries. Calculations for the lower symmetry structures albeit similar to the higher symmetry ones, were carried out so as not to rule out any low symmetry structures. The lowest energy structures, which are unique are shown in Fig. 1. We have carried out the optimizations for two structures with the  $D_{2d}$  symmetry in which the carbon dimers are oriented differently. We use a \* to distinguish between them. The one labeled as  $D_{2d}$  has a structure close to the  $C_{3v}$  structure and therefore is not shown in Fig. 1. Similarly, we have not shown the structure of the  $D_{2h}$  geometry since it is close to the  $T_h$  structure. Also, one of the  $T_d$  structures, labeled as  $T_d^*$  is close to the  $C_{3v}$  and therefore is not shown.

The geometry optimization has revealed the structure with  $C_{3v}$  symmetry to be the lowest energy structure among the structures considered here. The energies of all the calculated optimized structures relative to the energy of  $C_{3v}$  structure are given in Table I. We wish to point out here that a similar structure with  $T_d$  symmetry ( $T_d^*$ ) was found to be slightly higher in energy (0.13eV). The lower order of the  $C_{3v}$  symmetry group removes some of the degeneracies at the Fermi level. A fully unsymmetrized optimization leads to a structure lower in energy by only 0.01 eV. Therefore, we accept the  $C_{3v}$  structure as the lowest energy structure among the ones examined in this work. We believe that this structure is the same as the distorted  $T_d$  reported in Ref.<sup>19</sup>. The  $T_d$  and  $T_h$  structures shown in Fig. 1 are significantly higher in energy, respectively, by 14.94 and 14.5 eV than the  $C_{3v}$  structure. The energy difference between the  $T_d$  and  $T_h$  isomers is small (0.44 eV). The  $D_{2d}$  structure is also found to lie higher in energy by 0.06 eV than the  $C_{3v}$  structure. The other structures with  $D_{2d}^*$  and  $D_2$  symmetry are still higher by  $\sim 2$  eV.

To get more information about the stability of the different conformers, we have calculated the atomization energies and the vertical ionization potential (vIP) as well as the vertical electron affinities (vEA). These values, along with the magnetic moments, and the HOMO-LUMO gaps are summarized in Table I. We found that while the  $T_h$  structure has magnetic moment  $4 \mu_B$ , the other structures are found to possess a smaller magnetic moment of  $2 \mu_B$ . The calculated binding or atomisation energy of all the different structures are high which suggest that these clusters are highly stable. The vertical IP and EA are calculated by assuming the structure of the charged cluster to be same as the neutral one. The relative values of the vIP and vEA indicate the relative stability of the clusters with different geometry. Surprisingly, the higher energy isomers exhibit higher ionization potentials. The vertical IP of the  $T_d$ ,  $D_{2d}$  and the  $C_{3v}$  structures range between 4.51-4.61 eV. The earlier reported values of calculated vIP for the  $T_d$  structure ranges between 4.37 - 4.7 eV whereas the adiabatic IP is 4.43 eV<sup>13</sup>. The vIP or IP reported for other structures

are considerably higher than the experimental value. For the lowest energy structure with  $C_{3v}$  symmetry, we have calculated the adiabatic IP. In this case, the geometry of the charged cluster was allowed to relax. The calculated ionization potential (4.47 eV) is in excellent agreement with the recently determined value ( $4.4 \pm 0.02$  eV) from near threshold photoionization efficiency curves for the  $Ti_8C_{12}$ <sup>27</sup>.

The vertical electron affinity of the Ti Met-Cars were reported for  $T_d$  and  $T_h$  structures. While the experimental vertical electron affinity is  $1.16 \pm 0.05$  eV, the adiabatic affinity of  $1.05 \pm 0.05$  eV<sup>28</sup> is lower. The vEA calculated in the present work for the  $C_{3v}$ ,  $D_{2d}$  and  $T_d^*$  range between 0.89 - 1.08 eV. The vEA for other structures are relatively higher while the  $D_{2h}$  shows a very low vEA (Table I). The calculated adiabatic electron affinity of the  $C_{3v}$  structure is 1.00 eV which is in excellent agreement with the experimental value of 1.05 eV<sup>28</sup>. Apart from the  $C_{3v}$  anionic structure, we have optimized the geometries of the  $T_d^*$  and the  $D_{2d}$  structures also. The anionic  $T_d^*$  and  $C_{3v}$  are degenerate with an energy difference of 0.004 eV while the  $D_{2d}$  anion lies 0.015 eV above. The low electron affinity and the high ionization potential of the  $Ti_8C_{12}$  signifies the low reactivity of this cluster.

The energy ordering among the isomers and the good agreement with experimental IP and EA gives us confidence that  $C_{3v}$  structure is a likely candidate for the lowest energy structure within GGA.

Another possible way of identifying the structure will be through the infrared absorption spectrum. Recently, Heijnsbergen *et al.*<sup>18</sup> have carried out the measurement of infrared resonance-enhanced multiphoton ionization spectrum (IR-REMPI) of the  $Ti_8C_{12}$  clusters within the frequency range of  $400\text{ cm}^{-1}$  to  $1600\text{ cm}^{-1}$ . The IR-REMPI spectrum closely resembles the conventional infrared absorption spectrum in peak position and relative intensity. This experiment reports a broad peak of the IR-REMPI spectrum centered around  $1395\text{ cm}^{-1}$ . A comparison of the calculated spectrum with the measured spectrum can shed light on the possible candidate structures of the highly stable  $Ti_8C_{12}$  and also in identifying the Met-Cars in a mixed environment. The vibrational spectrum of the high lying structures with  $T_h$ ,  $T_d$ ,  $D_2$  and  $D_{2h}$  symmetries have several imaginary frequencies which further indicates these structures to be highly unstable. We, therefore, concentrate on the analysis of the vibrational modes and the IR and Raman spectrum of the two lowest energy structures, namely, the  $C_{3v}$  and  $D_{2d}$  structures. Pacheco *et al.*<sup>19</sup> have recently reported calculated IR absorption spectrum for the Met-Car with  $T_d$ ,  $T_h$  and  $D_{2d}$  structures and unsymmetric structures which are Jahn-Teller distorted. They have shown that while the Jahn-Teller distorted  $T_d$  structure is the lowest energy structure, the absorption spectrum of the  $D_{2d}$  structure matches the experimental spectrum best. They suggest that at finite temperature, the clusters with  $D_{2d}$  symmetry are most abundant. The calculated spectra in Ref.<sup>19</sup> were broadened by a Gaussian of FWHM of 40

$\text{cm}^{-1}$  which merges the closely spaced peaks. For the sake of completeness, we also calculated the IR spectra for the  $D_{2d}$  structure reported in Ref.<sup>19</sup>. The starting geometry differs from the other  $D_{2d}$  structure in the orientations of the carbon dimers. This structure, upon optimization, distorts largely from the starting geometry. The final structure is shown in Fig. 1 which we refer to as  $D_{2d}^*$ . This structure, although high in energy with respect to the  $C_{3v}$ , is stable with no imaginary frequency associated with it. However, the IR spectrum shows peaks at frequencies lower than in the experimental spectrum - one at  $1357\text{ cm}^{-1}$  and a much larger one at  $1310\text{ cm}^{-1}$ . Since this structure lies high in the energy scale, we concentrate on the IR spectra of the geometries labeled as  $C_{3v}$  and the  $D_{2d}$ .

Although both the  $C_{3v}$  and the  $D_{2d}$  symmetry groups are subgroups of the  $T_d$  symmetry group, they are independent. The small energy difference of 0.06 eV between them suggests the possibility of a symmetry breaking reaction path connecting the  $C_{3v}$  and  $D_{2d}$  structures. Indeed, there exists such a path shown in Fig. 2. The plot shows the small energy difference between the two structures. However, an estimate of the vibrational frequencies for such an anharmonic potential ruled out the possibility that at low or room temperature the Met-Cars can vibrate between the two structures. This fact again establishes that at zero temperature, it is likely to conform to the  $C_{3v}$  structure.

The experimental spectrum was measured between  $400 - 1600\text{ cm}^{-1}$  range. Therefore, we present our calculated spectrum in this frequency range in Fig. 3. The spectra shown in Fig. 3 in the upper two panels were broadened with a Gaussian of full width half maximum (FWHM) of  $6\text{ cm}^{-1}$  as well as  $40\text{ cm}^{-1}$ . The high resolution spectrum shows two clear peaks at  $1393\text{ cm}^{-1}$  and  $1442\text{ cm}^{-1}$  for the  $C_{3v}$  structure (Fig. 3, lower panel) while the  $D_{2d}$  structure shows peaks at  $1354\text{ cm}^{-1}$  and  $1393\text{ cm}^{-1}$ . At temperature  $T=0\text{ K}$ , both the structures have strong absorption peaks near  $1400\text{ cm}^{-1}$ . The smearing of the peaks with a gaussian of FWHM of  $40\text{ cm}^{-1}$  merges both the peaks and brings the spectra closer to the experimental one. In the experimental spectra, we detect a shoulder near  $1364\text{ cm}^{-1}$  which is clearly reproduced for the  $C_{3v}$  spectra but at a higher frequency. Although the shape of the IR absorption spectrum is correctly reproduced for the calculated  $C_{3v}$  spectra, the spectra is shifted slightly towards high energy region. The peaks of the  $D_{2d}$  spectra at  $1354$  and  $1393\text{ cm}^{-1}$  have comparable intensities and a smearing with Gaussian of FWHM of  $40\text{ cm}^{-1}$  does not show a shoulder clearly and the broad peak is to the left of the experimentally observed peak. In the low frequency region around  $500\text{ cm}^{-1}$ , the experimental spectrum shows peaks at  $455$  and  $520\text{ cm}^{-1}$ , which are correctly reproduced in case of  $C_{3v}$  structure and slightly shifted to higher frequency in case  $D_{2d}$  structure. Based on this observation and as well as the fact that the  $C_{3v}$  energy is lower than the  $D_{2d}$ , we believe that at temperature  $T=0\text{K}$  the IR spectrum will be dominated by

that of the  $C_{3v}$  structure. We have estimated the shift in the frequency of the highest peak of the  $C_{3v}$  structure due to the anharmonicity of the potential to be about  $10\text{ cm}^{-1}$ . These estimates also showed that the lowest eight excitations would encompass a broadening of nearly  $30\text{ cm}^{-1}$ .

Given that the experimental IR spectra was associated with clusters hot enough to undergo thermionic emission, the effect of thermal fluctuations will be strong in the experimentally measured IR spectra. Therefore a statistically weighted spectra of all the low-lying structure will better reproduce the experimental IR absorption spectrum. In Fig. 4, we show the weighted spectra of the  $C_{3v}$  and the  $D_{2d}$  structures which are within a range of 0.06 eV. In the Fig. 4, we show the calculated weighted IR absorption for temperatures  $T=300\text{K}$ ,  $750\text{K}$  and  $1100\text{K}$ . At room temperature, the spectra is dominated by the  $C_{3v}$  structure and weighted spectra has a peak shifted towards the high energy region. However, as the temperature is increased, the contribution from the  $D_{2d}$  structure increases and the spectra shows two close peaks for  $750\text{K}$ . At still higher temperature of  $1100\text{K}$ , the peak due to the  $C_{3v}$  is reduced. The noticeable feature is that the width of the experimental peak is better reproduced in the weighted spectra. The contribution from other isomers will become important at still higher temperature. Another noteworthy point is that the low energy region of the spectrum is better reproduced at room temperature.

For the purpose of comparison with any probable future experimental investigation, we also present our calculated Raman scattering spectra for both  $C_{3v}$  and  $D_{2d}$  geometries. This is the first calculated Raman spectra for  $\text{Ti}_8\text{C}_{12}$ . These plots are shown in Fig. 5. The Raman active modes are seen at lower frequencies which arises due to the Ti-Ti stretch mode and also twisting of the C-C bonds. These modes will change the volume of the cluster and hence the polarizability which will lead to Raman activities. The scattering intensities at high frequencies are low for both the structures. The spectra shown in Fig. 5 has been convoluted with a Gaussian of FWHM  $6\text{ cm}^{-1}$ . A larger value of FWHM will smear out most of the fine structures seen in the plots. A few weak peaks are seen in the region around  $1400\text{ cm}^{-1}$  where the IR activity is most strong. In the Raman spectra of both

the  $C_{3v}$  and  $D_{2d}$  structures, the most prominent peaks occur in the region between  $100$  to  $200\text{ cm}^{-1}$  which are nearly similar (Fig. 5). Therefore, Raman spectra in this low frequency region will not help in distinguishing the ground state structure between  $C_{3v}$  and  $D_{2d}$ . However, the spectra between  $300 - 600\text{ cm}^{-1}$  are distinguishable as can be seen from Fig. 5. A measurement of the Raman spectrum can greatly influence the debate over the equilibrium geometry of the Met-Cars.

#### IV. CONCLUSIONS

In conclusion, we have carried out extensive density functional calculations on the electronic structure and the vibrational states of the  $\text{Ti}_8\text{C}_{12}$  for different geometries. We find the geometry with  $C_{3v}$  symmetry to be the lowest energy structure. A study of the vibrational states show that the calculated IR absorption spectra for this geometry compares best with the experimental one. We find another structure with  $D_{2d}$  symmetry as a competing structure with an energy difference of only 0.06 eV. We find that a symmetry breaking reaction path exists from the  $D_{2d}$  to the  $C_{3v}$  structure. However, our estimates of the vibrational modes in the potential surface between the  $C_{3v}$  and  $D_{2d}$  ruled out any possibility of cold clusters vibrating between the two closely placed geometries. We estimate the reaction barrier to be about  $600\text{K}$ . We point out that the experiments may be associated with hot clusters and show that the overall width of the high frequency IR spectra supports a high temperature mixture of  $C_{3v}$  and  $D_{2d}$ . The two peak character observed in our calculations could reduce to a shoulder structure with small perturbation of IR intensity and peak positions. We also present our calculated Raman spectra for these two low-lying structures. An experimental measurement of the Raman spectra may help in deciding the ground state geometry of the  $\text{Ti}_8\text{C}_{12}$ .

#### V. ACKNOWLEDGEMENTS

TB and MRP were supported in part by ONR grant N0001400WX2011.

---

\* Corresponding author: FAX: +1-202-404-7546; e-mail: pederson@dave.nrl.navy.mil

<sup>1</sup> B. C. Guo, K. P. Kerns, A. W. Castleman, Jr., *Science* **255**, 1411 (1992).

<sup>2</sup> B. C. Guo, S. Wei, J. Purnell, S. A. Buzza, A. W. Castleman Jr., *Science* **256**, 515 (1992).

<sup>3</sup> S. Wei, B. C. Guo, H. T. Deng, K. Kerns, J. Purnell, S. A. Buzza, A. W. Castleman, Jr., *J. Am. Chem. Soc.* **116**, 4475 (1994).

<sup>4</sup> J. S. Pilgrim, and M. A. Duncan, *J. Am. Chem. Soc.* **115**, 6958 (1993).

<sup>5</sup> S. F. Cartier, B. D. May, A. W. Castleman, Jr., *J. Chem. Phys.* **100**, 5384 (1994).

<sup>6</sup> S. F. Cartier, B. D. May, A. W. Castleman, Jr., *J. Am. Chem. Soc.* **116**, 5295 (1994).

<sup>7</sup> H. T. Deng, B. C. Guo, K. P. Kerns, A. W. Castleman Jr., *Int. J. Mass Spec. Ion Proc.* **138**, 275 (1994).

<sup>8</sup> I. Dance, *J. Chem. Soc., Chem. Commun.* 1779 (1992).

<sup>9</sup> I. Dance, *J. Am. Chem. Soc.* **118**, 6309 (1996).

<sup>10</sup> H. Harris and I. Dance, *J. Phys. Chem. A* **105**, 3340 (2001).

<sup>11</sup> H. Chen, M. Feyereisen, X. P. Long, and G. Fitzgerald, *Phys. Rev. Letts.* **71**, 1732 (1993).

TABLE I: The energies of the clusters relative to the lowest energy structure, the atomisation energies ( $E_b$ ), spin and the HOMO-LUMO gap ( $\Delta$ ) of the  $Ti_8C_{12}$  clusters of various symmetries. All values are in eV.

	Relative energy	$E_b$	S	$\Delta$	vIP	vEA
$C_{3v}$	0.00	7.08	1	0.12	4.61	0.89
$T_h$	14.50	6.36	2	0.05	4.82	1.40
$T_d$	14.94	6.34	1	0.22	5.68	2.09
$T_d^*$	0.13	7.08	1	0.33	4.54	1.08
$D_{2d}$	0.06	7.08	1	0.13	4.51	0.93
$D_{2d}^*$	1.78	7.00	1	0.44	5.35	1.35
$D_{2h}$	14.47	6.36	1	0.25	6.26	0.66
$D_2$	1.99	6.99	1	0.07	5.18	1.53

- <sup>12</sup> Z. Lin and M. B. Hall, *J. Am. Chem. Soc.* **115**, 11165 (1993).
- <sup>13</sup> For a comprehensive review of the works on Met-Cars, see: M-M Rohmer, M. Bnard, and J-M. Poble, *Chem. Rev.* **100**, 495 (2000).
- <sup>14</sup> M. T. Bowers, *Acc. Chem. Res.* **27**, 324 (1994).
- <sup>15</sup> S. Lee, N. Gotts, G. von Helden, and M. T. Bowers, *Science* **267**, 999 (1995).
- <sup>16</sup> S. F. Cartier, Z. Y. Chen, G. J. Walder, C. R. Sleppy, and A. W. Castleman, Jr., *Science* **195**, 260 (1993).

- <sup>17</sup> R. Selvan and T. Pradeep, *Chem. Phys. Letts.* **149**, 309 (1999).
- <sup>18</sup> D. van Heijnsbergen, G. von Helden, M. A. Duncan, A. J. A. van Roij, and G. Meijer, *Phys. Rev. Letts.* **83**, 4983 (1999).
- <sup>19</sup> G. K. Gueorguiev and J. M. Pacheco, *Phys. Rev. Lett.* **99**, 115504-1 (2002).
- <sup>20</sup> P. Hohenberg and W. Kohn, *Phys. Rev.* **136**, B864 (1964); W. Kohn and L.J. Sham, *Phys. Rev.* **140**, A1133 (1965).
- <sup>21</sup> M. R. Pederson and K. A. Jackson, *Phys. Rev. B*, **41**, 7453 (1990); K. A. Jackson and M. R. Pederson, *Phys. Rev. B* **42**, 3276 (1990).
- <sup>22</sup> J. P. Perdew, K. Burke and M. Ernzerhof, *Phys. Rev. Lett.* **77**, 3865 (1996).
- <sup>23</sup> D. V. Porezag and M. R. Pederson, *Phys. Rev. B* **54** 9566 (1999).
- <sup>24</sup> M. R. Pederson and K. A. Jackson, *Phys. Rev. B* **41** 7453 (1990).
- <sup>25</sup> M. R. Pederson, D. V. Porezag, J. Kortus and D. C. Patton, *Phys. Status Solidi B* **217** 197 (2000).
- <sup>26</sup> D. Porezag and M. R. Pederson, *Phys. Rev. B* **54**, 7830 (1996).
- <sup>27</sup> H. Sakurai and A. W. Castleman Jr., *J. Phys. Chem. A* **102**, 10486 (1998).
- <sup>28</sup> L.-S. Wang, S. Li, H. Wu, *J. Phys. Chem.* **100**, 19211 (1996); S. Li, H. Wu, L. -S. Wang *J. Am. Chem. Soc* **119**, 7517 (1997).

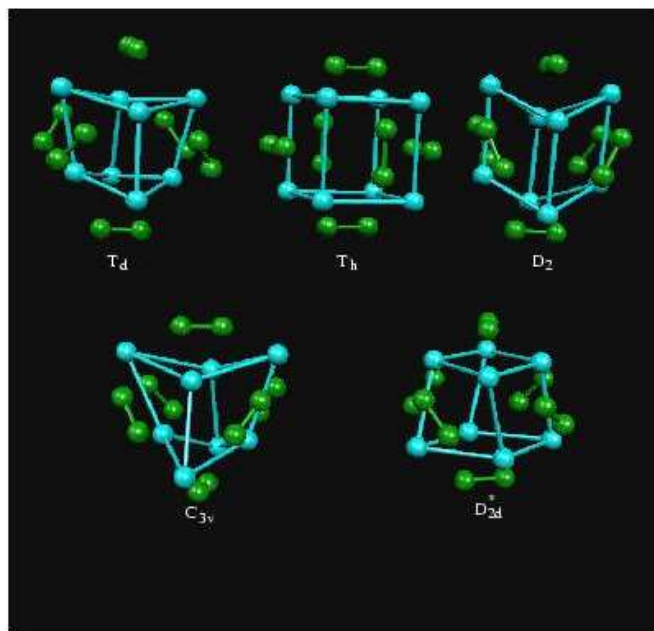


FIG. 1: The optimized geometries of the  $\text{Ti}_8\text{C}_{12}$  with various symmetries.

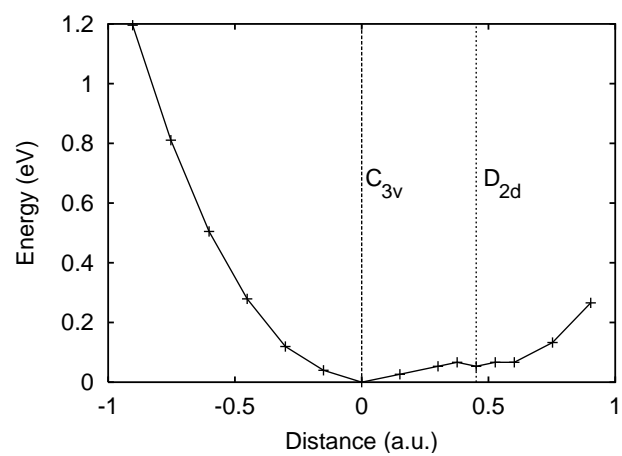


FIG. 2: A possible reaction path from the  $D_{2d}$  to the  $C_{3v}$  isomer. The x-axis shows the distances along the reaction path from the  $C_{3v}$  isomer.

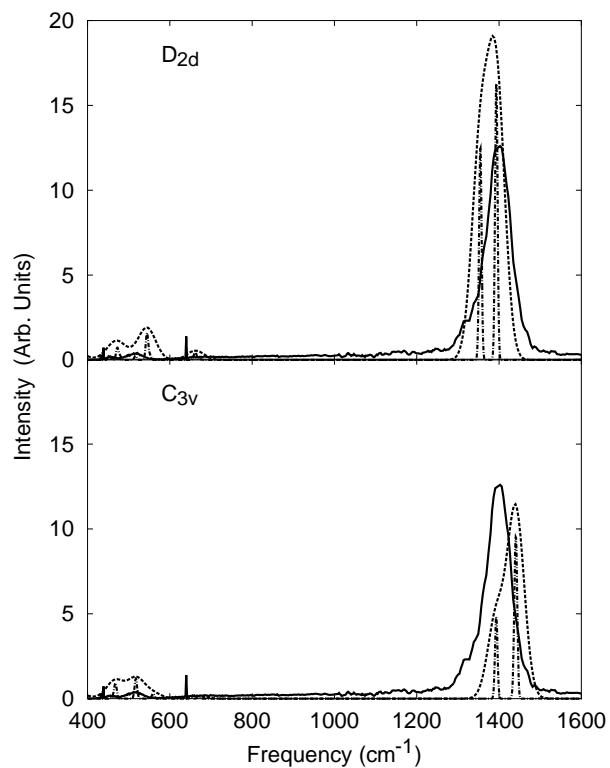


FIG. 3: The calculated IR intensities for  $\text{Ti}_8\text{C}_{12}$ . The upper panel shows the absorption spectra for  $D_{2d}$  geometry and the lower one shows the same for  $C_{3v}$  geometry. The solid lines represent the experimental spectra. The dash-dotted line shows the calculated spectra broadened with a gaussian of FWHM of  $6\text{ cm}^{-1}$  while the dashed line shows the one broadened with  $40\text{ cm}^{-1}$ . The convoluted curves are not renormalized. The theoretical intensities are in  $(\text{D}/\text{\AA})^2\text{amu}^{-1}$ . The experimental data are scaled down for comparison with theoretical data.

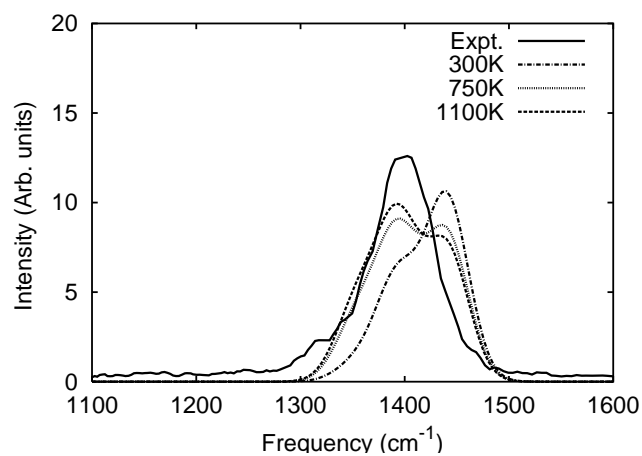


FIG. 4: The calculated IR intensities of the  $\text{Ti}_8\text{C}_{12}$  at different temperatures. The theoretical curves were convoluted with Gaussian of FWHM of  $40 \text{ cm}^{-1}$ .

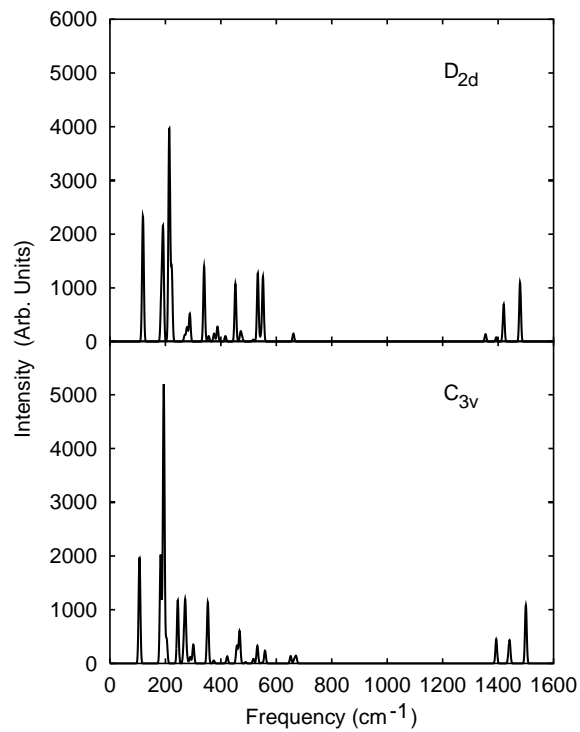


FIG. 5: The Raman scattering spectra of the low-lying  $\text{D}_{2d}$  and the  $\text{C}_{3v}$  structures. The spectra are broadened with a Gaussian of  $6 \text{ cm}^{-1}$ .